Analytic Potential Energy Functions for Simulating Aluminum Nanoparticles

Ahren W. Jasper, Nathan E. Schultz, and Donald G. Truhlar*

Department of Chemistry and Supercomputing Institute, University of Minnesota, Minneapolis, Minnesota 55455-0431

Received: November 12, 2004; In Final Form: January 7, 2005

Potential energy functions (PEFs) parametrized to bulk data are shown to perform poorly for small aluminum nanoparticles and clusters. In contrast, PEFs parametrized to a limited set of cluster and bulk data, but no nanoparticle data, perform well for nanoparticles. This validates a practical scheme for developing PEFs for nanoscale systems. Building on these findings, we optimized five PEFs by minimizing the error in the fit over a broad data set. Two of these PEFs have errors of less than or equal to 0.08 eV/atom for each of three categories of system sizes, i.e., for small clusters, for nanoparticles, and for bulk potential energies.

I. Introduction

Analytic representations of the forces governing nuclear motion (obtained as gradients of potential energy functions or PEFs) are much more affordable in simulations than direct electronic structure calculations of these forces, and analytic PEFs are especially practical for modeling nanoscale and bulk dynamics atomistically when one needs to adequately sample the initial conditions of the system or simulate long time scales. The increased efficiency is obtained at the cost of pre-validating the scheme for obtaining the analytic PEF.

PEFs may be validated by comparing the results of a simulation with some set of experimental results, but this approach is problematic for nanoparticles where experimental data is only recently becoming available (however rapidly) and where uncertainties in the experimental situation are precisely the questions for which atomistic simulations are hoped to provide insight. It is therefore often the case that analytic PEFs are parametrized against experimental data for the bulk, even when their eventual use is to model nanoscale or smaller systems. Because small clusters and nanoparticles have properties that are sometimes very different from those of bulk systems, this approach may not be reliable. Another difficulty with parametrization against experimental observations is that one cannot be certain that a PEF validated against one or more available experimental properties will be accurate for predicting a different property.

Alternatively, PEFs may be parametrized by fitting to the results of some set of higher-level theoretical calculations of the PEF itself. Nanoscale materials, however, are "large" from the point of view of high-level electronic structure calculations, limiting both the accuracy of individual calculations and also the number of geometries for which results may be obtained. The number of energetically accessible configurations in nanoparticles increases rapidly with system size (especially for high-temperature and nonequilibrium nanomaterials), making a comprehensive exploration of low-energy configurations with high-level methods difficult. PEFs obtained by fitting to a limited set of geometries may not be suitable for simulations involving geometries qualitatively different from those included in the data set.

The choice of functional forms for PEFs is an important consideration that can have a large effect on the success or failure of the parametrization. The "molecular mechanics" potentials based on valence stretches, bends, and torsions, van der Waals potentials, and Coulomb interactions between partial charges, that have been very successful in organic chemistry,[1−7] are not directly applicable to systems containing metals[8] with their variable valences and coordination numbers as high as twelve. The embedded atom[9] form, which—with minor revisions—goes under a variety of names (such as glue,[10,11] Finnis-Sinclair,[12] the second-moment approximation to tight binding,[13,14] and Sutton-Chen[15]), was found to be very successful for aluminum clusters[16] and will play a central role in the present article. Because the embedded atom form can be derived[17] by a second moment approximation to tight-binding molecular orbital theory, it is well justified theoretically for clusters and nanoparticles, as well as for bulk metals, for which it was originally intended. We will also consider several other functional forms, including pairwise, three-body, and many-body functional forms.

We have previously developed and systematically tested several analytic PEFs for subnano aluminum clusters.[16] The PEFs were tested using a data set[16,18] of ∼200 aluminum cluster energies for Al_N, where $N = 2$, 3, 4, 7, and 13, computed with the PBE0 hybrid density functional[19−21] and the MG3 basis set[22,23] as well as to the experimental face centered cubic (FCC) bulk cohesive energy[24] and lattice constant[25] (adjusted to remove finite temperature and zero-point energy effects[18,26]). Nineteen analytic PEFs that were parametrized for pure aluminum were obtained from the literature and tested,[16] and the most accurate of these PEFs was shown to have a mean unsigned error ϵ_c over the cluster energies in the data set of ∼0.12 eV/atom whereas the average value of ϵ_c for all 19 potentials was 1.7 eV/atom. Many of these PEFs were parametrized using only bulk data, and the PEFs from the literature that have errors in the FCC bulk cohesive energy of less than 0.1 eV/atom have an average ϵ_c of 0.8 eV/atom, which is too large for reliable simulations. We also reparametrized the literature PEFs and parametrized several newly proposed PEFs using the cluster data set.[16] Although the goal of that work was to develop PEFs for small clusters (up to Al_{13}), we also included the FCC bulk cohesive energy and lattice constant as fitting data. We tested

* Corresponding author. E-mail: truhlar@umn.edu.

10.1021/jp044805v CCC: $30.25
Published on Web 02/11/2005

the ability of a total of 32 functional forms to fit the cluster and bulk data, and the best of the resulting reparametrized PEFs had $\epsilon_c \approx 0.05$ eV/atom and even smaller errors for the FCC bulk cohesive energy.

In this work, we present an expanded data set that includes nanoparticle structures up to Al_{177}, and we test the effectiveness of the fitting strategy presented above for predicting nanoparticle energies on the basis of interpolating between small clusters and the bulk. Finally, a set of multidomain PEFs, i.e., PEFs capable of accurately modeling small clusters, nanoparticles, and bulk aluminum, is presented.

II. Nanoparticle Data Set

The nanoparticle data set includes the cluster data discussed above, as presented previously.[16,18] That data set is augmented with 347 additional Al_3 geometries consisting of bond angle curves where two of the atom−atom distances R_1 and R_2 are fixed and the interior bond angle is varied from 15 to 175° in 10° intervals; twenty-one curves are included with the values $R_1 \le R_2 = 2.0$, 2.3, 2.51, 2.86, 3.5, and 5.0 Å. Twenty additional Al_4 geometries are included that correspond to torsions away from the minimum-energy Al_4 geometry (a rhombus with the four perimeter atom−atom distances equal to 2.55 Å), as well as torsions of a trapezoid constructed using the same atom−atom distance for the three smallest atom−atom distances. Several Al_{13} geometries are included: the optimized FCC, hexagonal close packed (HCP), and icosahedral structures, a Jahn−Teller distorted icosahedral cluster, a geometry formed by making a 30° twist to $^1/_2$ of the FCC structure (corresponding to a geometry intermediate along an FCC/HCP transition), FCC and HCP structures formed using the 298 K lattice spacings, and thirty disordered Al_{13} clusters including some geometries with over-coordinated atoms (i.e., atoms with more than twelve close neighbors). Also included are ten disordered Al_{19} clusters, two disordered Al_{43} clusters, and optimized geometries for Al_{14} to Al_{25}.

To generate nanoparticle geometries for the data set, we consider quasispherical clusters (QSCs), which are defined as follows. An FCC, HCP, body-centered cubic (BCC), or simple cubic (SC) crystal is generated by surrounding a central atom using some lattice parameter (or, for the HCP crystal, set of lattice parameters). The distance from the central atom to some other atom in the cluster i is denoted R_i, and due to the regular nature of the crystals the set of R_i consists of a much smaller set of unique values S_m. The mth QSC for each type of crystal is defined as containing all of the atoms with $R_i \le S_m$. Series of QSCs using the 298 K lattice spacings are included in the data set for FCC ($N = 19-177$), HCP ($N = 19-135$), and BCC ($N = 15-133$) crystals, where N is the number of atoms in the QSC. Several FCC QSCs were optimized and included in the data set. Similar series were calculated for clusters with the central atom removed, i.e., with an interior vacancy. Also included are QSCs with geometries where the lattice constants are varied around their minimum-energy values. Equilibrium lattice constants for the HCP, BCC, and SC structures were taken from the PBE[19] density functional theory calculations of Jaffe et al.[27]

In summary, a total of 601 new geometries are included, and 127 of the new geometries have $N \ge 20$. A quasispherical FCC cluster Al_N with $N = 19$ has a diameter of ~1 nm, and we define particles with $N = 2-19$ as clusters, and those with $N = 20-177$ as (small) nanoparticles. FCC quasispherical clusters with $N = 13$, 55, and 177 have approximate diameters of 0.85, 1.4, and 2.0 nm, respectively, and these cluster sizes correspond to complete first, second, and third shells around a central atom.

The PBE0/MG3 method[19−23] was used to compute energies for $N \le 13$, and the recently developed[28] effective core method PBE0/MEC was used for $N > 13$. The PBE0/MG3 method was validated[18] against more accurate calculations for $N = 2-7$ and was shown to be accurate to ~0.01 eV/atom. The PBE0/MEC method was shown[28] to agree well with all-electron PBE0/MG3 results for $N = 2-13$ with an average unsigned deviation of 0.02 eV/atom. Calculations were carried out using the GAUSSIAN03[29] and NWChem[30] programs.

For the purposes of evaluating the analytic PEFs, the data set is divided into eleven groups based on cluster size. The groups contain particles with sizes $N = 2$, 3, 4, 7, 9−13, 14−19, 20−43, 50−55, 56−79, 80−87, and 89−177, respectively, and are labeled by their average particle size $\bar{M}$, where $\bar{M} = 2$, 3, 4, 7, 13, 18, 33, 53, 71, 86, and 124, respectively. The number of data points in each group is 44, 402, 79, 42, 72, 42, 46, 23, 27, 15, and 16.

In performing fits and computing errors, we use a set of weights w_i that weight particles with compressed atom−atom distances (and therefore with high energies) less than geometries that are more energetically favorable:

$$w_i = \begin{cases} 1 & \text{for } R_i \ge R_{nc} \\ V_2(R_{nc})/V_2(R_i) & \text{for } R_i < R_{nc} \end{cases} \quad (1)$$

where R_i is the smallest atom−atom distance in the cluster, and V_2 is the energy of the diatomic two-body interaction energy relative to the energy of two separated atoms. The set of geometries where $R_i > R_{nc}$ defines a subset with no close contacts, and each geometry in this subset is given full weight. We chose R_{nc} such that $V_2(R_{nc}) = -V_2(R_e) = 1.55$ eV, where R_e is the equilibrium distance of Al_2. Thus $R_{nc} = 1.82$ Å. The smallest value of R_i in the data set is 0.91 Å, and the particle with this R_i has a weight of 0.008. Of the 808 geometries in the data set, 761 have $w_i = 1$, and 27 have $0.01 \le w_i < 1$.

For each PEF, the following errors are computed. The accurate energy and the energy predicted by the PEF for each geometry i are labeled E_i and F_i, respectively. The unsigned error per atom for any data point is

$$\Delta E_i = |E_i - F_i|/N_i \quad (2)$$

where N_i is the number of atoms in geometry i. The error per atom in the energy difference of any pair of geometries is

$$\Delta\Delta E_{ij} = |(E_i - E_j) - (F_i - F_j)|/N_i \quad (3)$$

for $N_i = N_j$, and $\Delta\Delta E_{ij}$ is not defined for $N_i \ne N_j$. The mean unsigned error (MUE) per atom for each group $\bar{M}$ is defined by

$$\epsilon_{\bar{M}} = \frac{\langle w_i \Delta E_i \rangle_i^{(\bar{M})}}{\langle w_i \rangle_i^{(\bar{M})}} + \frac{\langle w_i w_j \Delta\Delta E_{ij} \rangle_{ij}^{(\bar{M})}}{\langle w_i w_j \rangle_{ij}^{(\bar{M})}} \quad (4)$$

where w_i is a weight, $\langle \cdots \rangle_{ij}^{(\bar{M})}$ denotes an average over all pairs of particles with the same number of atoms in group $\bar{M}$, and $\langle \cdots \rangle_i^{(\bar{M})}$ denotes an average of all particles in group $\bar{M}$.

We also consider the performance of the various PEFs for bulk FCC, HCP, and BCC crystals. Accurate FCC lattice constants, bulk moduli, and cohesive energies were taken from experiment,[18,24−26] and for the HCP and BCC crystals, bulk data were obtained from the PBE density functional theory calculations of Jaffe et al.,[27] with the HCP and BCC cohesive energies scaled by the ratio of the experimental and calculated FCC cohesive energies. These data were used along with the

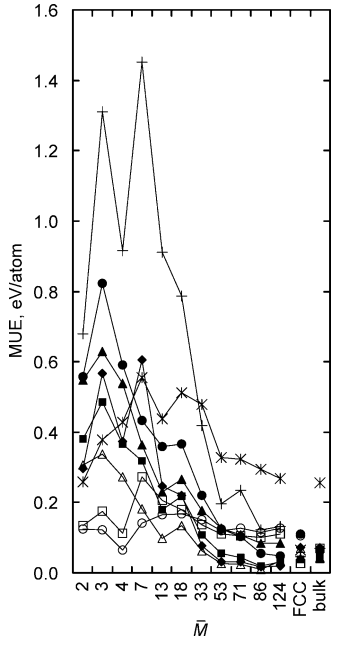

Figure 1. MUEs per atom ϵ_M for each group of data $\bar{M}$, ϵ_{FCC}, and ϵ_{bulk} for several PEFs parametrized using mainly bulk data (refs 15 and 33−40), where the label denotes the source of the functional form: GoI (open circles), BetH (open triangles), PapCEP (open squares), SutC (filled circles), MeiD (filled triangles), StrM (filled squares), MisFMP (filled diamonds), deSPH/M (asterisks), CoxJM (pluses).

Murnaghan-Birch equation of state[31,32] to approximate the FCC, HCP, and BCC bulk potential energies per atom at atomic volumes of 13, 15, and 18 Å^3 as well as at the atomic volumes corresponding to the experimental (for FCC) or calculated (for HCP and BCC) minimum-energy volume for each crystal (16.3, 16.8, and 17.0 Å^3 for FCC, HCP, and BCC, respectively). We define the mean unsigned error ϵ_{bulk} of bulk binding energies as the average of the unsigned errors (per atom) with respect to these twelve data. Note that the bulk energies defined are relative to isolated atoms, and the minimum bulk potential energy for each crystal corresponds to the zero-point exclusive cohesive energy for that crystal. Several of the PEFs considered in this article were originally fit[33−40] using the experimental FCC cohesive energy, and we denote the error in the bulk FCC energy evaluated at the experimental atomic volume by ϵ_{FCC}. The energy differences between the bulk phases is relatively small; the PBE96-GGA calculations predict the FCC−HCP and FCC−BCC energy differences to be ∼0.05 and ∼0.10 eV, respectively.

III. Results

Several analytic PEFs from our previous study[1] and elsewhere in the literature were tested using the nanoparticle data set discussed above. Of the PEFs that were collected and described in ref 16 but originally parametrized elsewhere, nine have errors in the FCC bulk cohesive energy ϵ_{FCC} of ∼0.1 eV or less. These include: seven embedded-atom PEFs (which we label by their authors' names, i.e., GoI,[33] SutC,[15] MeiD,[34] StrM,[35] BetH,[36] MisFMP,[37] and PapCEP[38]), one pairwise additive PEF (deSPH/M[39]), and one PEF that may be written as the sum of two-body and three-body interactions (CoxJM[40]). Some cluster data (specifically, data for Al_6) was included in the parametrization[39] of the deSPH/M PEF, but otherwise only bulk data was used to fit these nine PEFs.

Errors were computed using eq 4 for these nine PEFs and are plotted in Figure 1, along with ϵ_{FCC} and ϵ_{bulk}. Though most of the PEFs in Figure 1 were fit to experimental FCC data, most of them have ϵ_{bulk} values (which include HCP and BCC data) that are similar in magnitude to their ϵ_{FCC} values. However, the deSPH/M PEF does poorly for the HCP and BCC bulk systems, and only the MisFMP PEF predicts the correct ordering of the crystal phases. For most PEFs, the values of ϵ_M for $\bar{M} = 53-124$ (i.e., for particles larger than Al_{43}) are typically comparable with the error in the FCC bulk cohesive energy. The GoI PEF[19] has one of the largest values of ϵ_{FCC} (0.10 eV) of the PEFs plotted in Figure 1, but the error per atom does not increase dramatically for nanoparticles and clusters; the maximum error for any one of the data groups for this PEF is 0.16 eV per atom. For the remaining embedded-atom PEFs, the error increases more significantly for $\bar{M} = 2-33$ (by as much as factors of 6−20). For the CoxJM PEF, the error for $\bar{M} = 71-124$ increases somewhat (by ∼0.15 eV per atom) compared to the error in the bulk but remains fairly constant over those groups. The error again increases dramatically for smaller clusters, and for this PEF the break occurs toward slightly larger clusters (around Al55). The deSPH/M pairwise additive PEF has an error that is fairly constant over the data set, but its magnitude is much larger than the error in the bulk FCC cohesive energy even for the biggest nanoparticles in the data set.

The overall trend in the data in Figure 1 demonstrates that PEFs fit mainly to bulk data perform poorly for clusters and nanoparticles smaller than approximately Al_{55}. Al_{55} is the smallest FCC QSC with two complete atomic shells, and only ∼25% of the atoms in an Al_{55} FCC QSC are coordinated to twelve atoms (the bulk coordination number for Al). It is therefore interesting to note that the filling of the second shell seems to serve as a delimiter between the bulklike and nonbulklike regimes.

As discussed above, we have previously[16] parametrized several PEFs to a data set consisting of cluster energies for Al_N, $N = 2-13$, and only two pieces of bulk data (the FCC cohesive energy and lattice constant); the bulk data were given a weight of 20% that of the cluster data. We will refer to this as the cluster data set and to PEFs parametrized in this way as "cluster-parametrized" PEFs.

In Figure 2, errors are plotted for the cluster-parametrized PEFs with the same functional forms presented in Figure 1. No bulk HCP and BCC data were used in these parametrizations, and, as stated in the previous paragraph, bulk FCC data were given a small weight; therefore, ϵ_{FCC} and ϵ_{bulk} occasionally increase slightly compared to the parametrization in Figure 1. The overall error in the only pairwise additive PEF considered (deSPH/M) is not improved compared to its original bulk parametrization. For the other functional forms, however, the cluster-parametrized PEFs are much more accurate than the PEFs parametrized only to bulk data, even for particle sizes that were not included in the parametrization (i.e., for Al_{14} to Al_{177}, or equivalently for $\bar{M} = 18-124$). This is true even when the error for the bulk increases, as is the case for the StrM functional form. The best cluster-parametrized PEFs have error distributions that are similar to one another and that are fairly constant over the various data groups. Compared to the errors in Figure 1, the errors improve on average by factors of 5 and 2 for $\bar{M} = 2-13$ and 18−124, respectively. The absolute errors for the best PEFs are less than ∼0.1 eV per atom, which provides our first key conclusion, namely that *PEFs that are accurate for nanoparticle systems may be obtained by fitting to a limited set of cluster and bulk data*. Furthermore, this strategy is shown to be successful for a variety of different functional forms. Also shown in Figure 2 is the SCN PEF, which

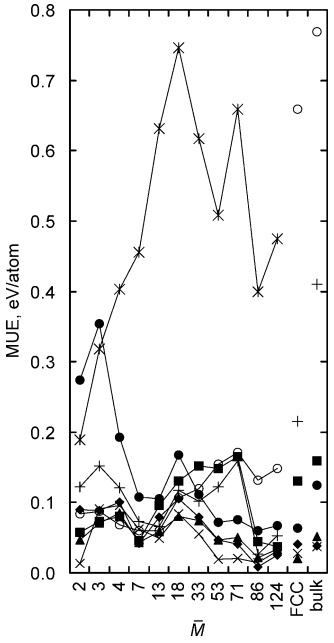

Figure 2. MUEs per atom ϵ_M for each group of data $\bar{M}$, ϵ_{FCC}, and ϵ_{bulk} for several PEFs parametrized using the cluster data set and FCC bulk data (ref 16). The labels are the same as those used in Figure 1, and the SCN PEF (x) is also shown. Note that the PapCEP, BetH, and Gol PEFs have equivalent functional forms and are represented by a single curve (open circles).

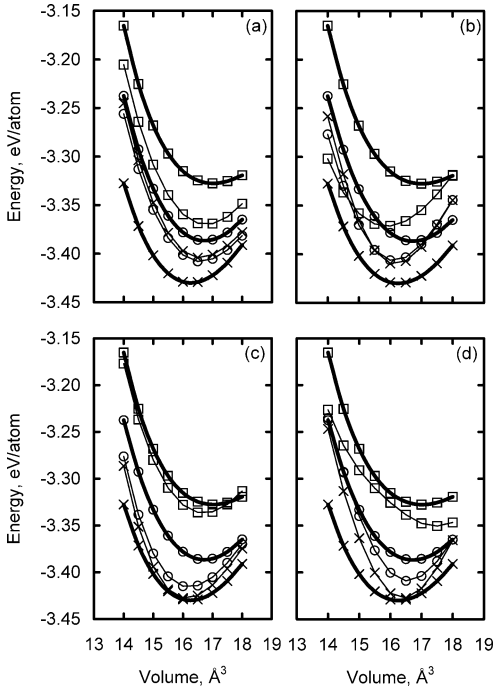

Figure 3. Energies per atom for bulk FCC (x), HCP (circles), and BCC (squares) crystals. Accurate energies are shown as thick solid lines, and fitted energies are shown as thin lines for the (a) cluster parametrized SCN, (b) cluster parametrized MeiD, (c) NP-A, and (d) N-B PEFs.

was not previously fit mainly to bulk data and therefore is not shown in Figure 1.

We now consider the four PEFs from Figure 2 that have average values of $\epsilon_M < 0.10$ eV/atom, specifically the ones based on the SCN, MeiD, MisFMP, and StrM functional forms. We also consider the Gol functional form because it is widely used and represents a simple version of the embedded-atom formalism. The cluster-parametrized SCN, MeiD, and MisFMP PEFs have average values of ϵ_M of ~0.06 eV/atom, and the cluster-parametrized StrM and Gol PEFs have average values of ϵ_M of ~0.10 eV/atom. These PEFs are accurate for clusters, nanoparticles, and the FCC bulk cohesive energy. However, they perform poorly for the bulk HCP and BCC crystal structures, which were not included in the cluster parametrizations, as shown in Figure 3a,b for the cluster parametrized SCN and MeiD PEFs, respectively.

We can further refine these five PEFs using the full nanoparticle data set and using bulk FCC, HCP, and BCC energies by minimizing the sum of ϵ_{bulk} and the average value of ϵ_M. Extra weight was given to the FCC cohesive energy. The improved nanoparticle potentials are named NP-A, NP-B, NP-C, NP-D, and NP-E, respectively, as indicated in Table 1. The error distributions for these multidomain-size potentials are shown in Figure 4, and the bulk potential energy curves for the two best PEFs (NP-A and NP-B) are shown in Figure 3c,d, respectively. The fitted values of the bulk properties along with the MUEs for the cluster and nanoparticle data in the data set are shown in Table 1. The NP potentials based on the MisFMP and Gol functional forms do not reproduce the correct ordering of bulk crystal types, and the remaining functional forms underestimate the difference in the FCC and HCP cohesive energies. The Gol functional form lacks the functionality to reproduce the bulk FCC−HCP energy difference; the MisFMP functional form is able to model this behavior,[37] but not when nanoparticle and cluster data are included in the fitting procedure.

Our second key conclusion is that *we can obtain functions with good accuracy for nanoparticles that also predict accurate cluster properties and the correct ordering of bulk phases*. In particular, we accomplish this with the MeiD and SCN functional forms (i.e., the NP-A and NP-B PEFs), which accurately reproduce the ordering of bulk crystal types, have small errors over the cluster and nanoparticle data, and ac-

TABLE 1: Bulk Lattice Constants, Bulk Cohesive Energies, and Mean Unsigned Errors Per Atom (MUE) for Five PEFs (Distances in Å; Energies in eV)

		FCC		HCP[b]		BCC		MUE			
PEF	func form[a]	l.c.	E_c	l.c.	E_c	l.c.	E_c	l.c.	E_c	cluster[c]	nano[d]
accurate[e]		4.02	3.43	2.87	3.39	3.24	3.33				
NP-A	SCN[f] (16)	4.01	3.43	2.84	3.42	3.22	3.34	0.02	0.01	0.06	0.03
NP-B	MeiD (34)	4.03	3.43	2.86	3.41	3.27	3.35	0.02	0.02	0.08	0.04
NP-C	StrM (35)	4.00	3.43	2.83	3.42	3.18	3.37	0.04	0.03	0.08	0.11
NP-D	Gol (33)	4.01	3.43	2.84	3.43	3.19	3.41	0.03	0.04	0.12	0.05
NP-E	MisFMP (37)	4.01	3.43	2.85	3.44	3.21	3.44	0.02	0.06	0.18	0.08

[a] The functional form is denoted by acronyms based on the names of the authors who obtained fits for pure Al. References are given in parentheses. [b] The ideal HCP structure is used (i.e., the lattice constants are related by $c/a = \sqrt{8/3}$), and a is tabulated. [c] MUE for clusters with 2−19 atoms. [d] MUE for nanoparticles with 20−177 atoms. [e] Experimental data for the bulk FCC crystal; scaled PBE96-GGA data from ref 27 for the HCP and BCC crystals. [f] This functional form was named ER2+ESCNa in ref 16.

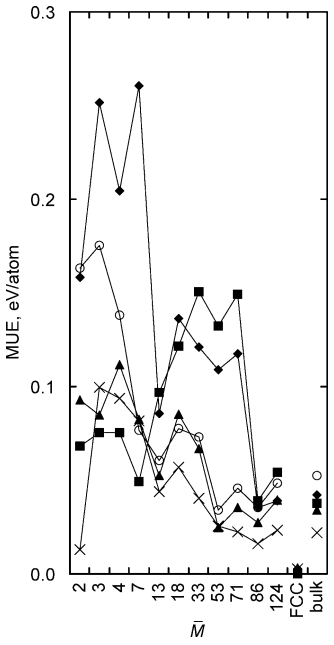

Figure 4. MUEs per atom ϵ_M for each group of data $\bar{M}$, ϵ_{FCC}, and ϵ_{bulk} for several PEFs parametrized using the full data set and FCC, HCP, and BCC bulk data (present work). The labels are the same as those used in Figures 1 and 2.

curately predict the bulk FCC energy and FCC, HCP, and BCC lattice constants. Unfortunately, the HCP crystal is too strongly bound (by 0.02−0.03 eV/atom) in both cases. Nevertheless these two potentials both do very well. The NP-A potential based on the SCN form is slightly more accurate, but the N-B potential based on the MeiD form is much less expensive to evaluate in simulations, and both are recommended.

IV. Concluding Remarks

We have presented a scheme for parametrizing analytic PEFs for nanoparticle systems that uses a limited set of bulk data and electronic structure calculations for small clusters. The scheme was validated using pure aluminum systems but should be applicable to other materials as well. Several different analytic PEFs with various functional forms that were parametrized for aluminum in this way were shown to accurately reproduce the results of hybrid density functional theory calculations for nanoparticles (1−2 nm) that were not included in the parametrization data set. Finally, we have obtained a set of five universal PEFs whose parameters were optimized using the full nanoparticle data set with geometries for Al_N, $N = 2-177$ and bulk data for FCC, HCP, and BCC crystals. This study represents the first example of analytic PEFs validated against accurate calculations for metal nanoparticles, and it opens a new window of modeling applications. All of the PEFs considered here may be obtained as FORTRAN subroutines on the Internet.[41]

Acknowledgment. This work is supported in part by the Defense-University Research Initiative in Nanotechnology (DURINT) of the U.S. Army Research Laboratory and the U.S. Army Research Office under agreement number DAAD190110503. Computational resources were provided by the Minnesota Supercomputing Institute and by a Grand Challenge Grant at Pacific Northwest National Laboratories.

Supporting Information Available: Geometries and accurate (PBE0/MG3 and PBE0/MEC) energies for the 808 data that comprise the nanoparticle data set, plus the parameters for the two best PEFs, i.e., NP-A and NP-B. This material is available free of charge via the Internet at http://pubs.acs.org.

References and Notes

(1) Bowen J. P.; Allinger, N. L. *Rev. Comput. Chem.* **1991**, *2*, 81.
(2) Dinur, U.; Hagler, A. T. *Rev. Comput. Chem.* **1991**, *2*, 99.
(3) Hagler, A. T.; Ewig, C. S. *Comput. Phys. Commun.* **1997**, *84*, 131.
(4) Pearlman, D. A.; Case, D. A.; Caldwell, J. W.; Ross, W. S.; Cheatham, T. E., III; DeBolt, S.; Ferguson, D.; Seibel, G.; Kollman, P. *Comput. Phys. Commun.* **1995**, *91*, 1.
(5) Cornell, W. D.; Cieplak, P.; Bayly, C. I.; Gould, I. R.; Merz, K. M.; Ferguson, D. M.; Spellmeyer, D. C.; Fox, T.; Caldwell, J. W.; Kollman, P. A. *J. Am. Chem. Soc.* **1995**, *117*, 5179.
(6) Brooks, B. R.; Bruccoleri, R. E.; Olafson, B. D.; States, D. J.; Swaminathan, S.; Karplus, M. *J. Comput. Chem.* **1983**, *4*, 187.
(7) MacKerell, A. D., Jr.; Brooks, B.; Brooks, C. L., III; Nilsson, L.; Roux, B.; Won, Y.; Karplus, M. In *The Encyclopedia of Computational Chemistry*; Schleyer, P. v. R., Allinger, N. L., Clark, T., Gasteiger, J., Kollman, P. A., Schaefer, H. F., III, Schreiner, P. R., Eds.; John Wiley & Sons: Chichester, U.K., 1998; Vol. 1, pp 271−277.
(8) Landis, C. R.; Root, D. M.; Thomas, C. *Rev. Comput. Chem.* **1995**, *6*, 73.
(9) Daw, M. S.; Baskes, M. I. *Phys. Rev. Lett.* **1983**, *50*, 1285; *Phys. Rev. B* **1984**, *29*, 6443. Foiles, S. M. *Phys. Rev. B* **1985**, *32*, 7685. Foiles, S. M.; Baskes, M. I.; Daw, M. S. *Phys. Rev. B* **1986**, *33*, 7983.
(10) Ercolessi, F.; Parrinello, M.; Tosatti, E. *Philos. Mag. A* **1988**, *58*, 213.
(11) Nishitani, S. R.; Ohgushi, S.; Inoue, Y.; Adachi, H. *Mater. Sci. Eng.* **2001**, *A309*−*310*, 490.
(12) Finnis, M. W.; Sinclair, J. E. *Philos. Mag. A* **1984**, *50*, 45.
(13) Gupta, R. P. *Phys. Rev. B* **1985**, *23*, 6265.
(14) Tomànek, D.; Aligia, A. A.; Balseiro, C. A. *Phys. Rev. B* **1985**, *32*, 5051.
(15) Sutton, A. P.; Chen, J. *Philos. Mag. Lett.* **1990**, *61*, 139.
(16) Jasper, A. W.; Staszewski, P.; Staszewska, G.; Schultz, N. E.; Truhlar, D. G. *J. Phys. Chem. B* **2004**, *108*, 8996.
(17) Ackland, G. J.; Finnis, M. W.; Vitek, V. *J. Phys. F: Met. Phys.* **1988**, *18*, L153.
(18) Schultz, N. E.; Staszewska, G.; Staszewski, P.; Truhlar, D. G. *J. Phys. Chem. B* **2004**, *108*, 4850.
(19) Perdew, J. P.; Burke, K.; Ernzerhof, M. *Phys. Rev. Lett.* **1996**, *77*, 3865; **1997**, *78*, 1396(E).
(20) Ernzerhof, M.; Scuseria, G. E. *J. Chem. Phys.* **1999**, *110*, 5029.
(21) Adamo, C.; Barone, V. *J. Chem. Phys.* **1999**, *110*, 6158.
(22) Fast, P. L.; Sanchez, M. L.; Truhlar, D. G. *Chem. Phys. Lett.* **1999**, *306*, 407.
(23) Curtiss, L. A.; Redfern, P. C.; Raghavachari, K.; Rassolov, V.; Pople, J. A. *J. Chem. Phys.* **1999**, *110*, 4703.
(24) *Selected Values of the Thermodynamic Properties of the Elements*; Hultgren, R., Desai, P. D., Hawkins, D. T., Gleiser, M., Kelly, K. K., Wagman, D. D., Eds.; American Society for Metals: Metals Park, OH, 1973.
(25) *American Institute of Physics Handbook*, 3rd ed.; Zemansky, M. W., Gray, D. E., Eds.; McGraw-Hill Book Company: New York, 1972.
(26) Gaudoin, R.; Foulkes, W. M. C. *Phys. Rev. B* **2002**, *66*, 052104.
(27) Jaffe, J. E.; Kurtz, R. J.; Gutowski, M. *Comput. Mater. Sci.* **2000**, *18*, 199.
(28) Schultz, N. E.; Truhlar, D. G. *J. Chem. Theory Comput.* **2005**, *1*, 41.
(29) Frisch, M. J.; Trucks, G. W.; Schlegel, H. B.; Scuseria, G. E.; Robb, M. A.; Cheeseman, J. R.; Montgomery, J. A.; Vreven, T.; Kudin, K. N.; Burant, J. C.; Millam, J. M.; Iyengar, S. S.; Tomasi, J.; Barone, V.; Mennucci, B.; Cossi, M.; Scalmani, G.; Rega, N.; Petersson, G. A.; Nakatsuji, H.; Hada, M.; Ehara, M.; Toyota, K.; Fukuda, R.; Hasegawa, J.; Ishida, M.; Nakajima, T.; Honda, Y.; Kitao, O.; Nakai, H.; Klene, M.; Li, X.; Knox, J. E.; Hratchian, H. P.; Cross, J. B.; Adamo, C.; Jaramillo, J.; Gomperts, R.; Stratmann, R. E.; Yazyev, O.; Austin, A. J.; Cammi, R.; Pomelli, C.; Ochterski, J. W.; Ayala, P. Y.; Morokuma, K.; Voth, G. A.; Salvador, P.; Dannenberg, J. J.; Zakrzewski, V. G.; Dapprich, S.; Daniels, A. D.; Strain, M. C.; Farkas, O.; Malick, D. K.; Rabuck, A. D.; Raghavachari, K.; Foresman, J. B.; Ortiz, J. V.; Cui, Q.; Baboul, A. G.; Clifford, S.; Cioslowski, J.; Stefanov, B. B.; Liu, G.; Liashenko, A.; Piskorz, P.; Komaromi, I.; Martin, R. L.; Fox, D. J.; Keith, T.; Al-Laham, M. A.; Peng, C. Y.; Nanayakkara, A.; Challacombe, M.; Gill, P. M. W.; Johnson, B.; Chen, W.; Wong, M. W.; Gonzalez, C.; Pople, J. A. *Gaussian03*, version B.05; Gaussian Inc.: Pittsburgh, PA, 2003.
(30) Straatsma, T. P.; Aprà, E.; Windus, T. L.; Bylaska, E. J.; de Jong, W.; Hirata, S.; Valiev, M.; Hackler, M. T.; Pollack, L.; Harrison, R. J.; Dupuis, M.; Smith, D. M. A.; Nieplocha, J.; Tipparaju V.; Krishnan, M.; Auer, A. A.; Brown, E.; Cisneros, G.; Fann, G. I.; Fruchtl, H.; Garza, J.; Hirao, K.; Kendall, R.; Nichols, J.; Tsemekhman, K.; Wolinski, K.; Anchell, J.; Bernholdt, D.; Borowski, P.; Clark, T.; Clerc, D.; Dachsel, H.; Deegan,

M.; Dyall, K.; Elwood, D.; Glendening, E.; Gutowski, M.; Hess, A.; Jaffe, J.; Johnson, B.; Ju, J.; Kobayashi, R.; Kutteh, R.; Lin, Z.; Littlefield, R.; Long, X.; Meng, B.; Nakajima, T.; Niu, S.; Rosing, M.; Sandrone, G.; Stave, M.; Taylor, H.; Thomas, G.; van Lenthe, J.; Wong, A.; Zhang, Z. *NWChem*, version 4.6; Pacific Northwest National Laboratory, Richland, WA 99352-0999, USA; 2003. Kendall, R. A.; Aprà, E.; Bernholdt, D. E.; Bylaska, E. J.; Dupuis, M.; Fann, G. I.; Harrison, R. J.; Ju, J.; Nichols, J. A.; Nieplocha, J.; Straatsma, T. P.; Windus, T. L.; Wong, A. T. *Computer Phys. Commn.* **2000**, *128*, 260−283.

(31) Murnaghan, F. D. *Proc. Natl. Acad. Sci. U.S.A.* **1944**, *30*, 244.

(32) Birch, F. *J. Geophys. Res.* **1952**, *57*, 227.

(33) Gollisch, H. *Surf. Sci.* **1986**, *166*, 87.

(34) Mei, J.; Davenport, J. W. *Phys. Rev. B* **1992**, *46*, 21.

(35) Streitz F. H.; Mintmire, J. W. *Phys. Rev. B* **1994**, *50*, 11996.

(36) Betz, G.; Husinsky, W. *Nucl. Instrum. Methods B* **1997**, *122*, 311.

(37) Mishin, Y.; Farkas, D.; Mehl, M. J.; Papaconstantopoulos, D. A. *Mater. Res. Soc. Symp. Proc.* **1999**, *538*, 535.

(38) Papanicolaou, N. I.; Chamati, H.; Evangelakis, G. A.; Papaconstantopoulos, D. A. *Comput. Mater. Sci.* **2003**, *27*, 191.

(39) de Sainte Claire, P.; Peslherbe, G. H.; Hase, W. L. *J. Phys. Chem.* **1995**, *99*, 8147.

(40) Cox, H.; Johnston, R. L.; Murrell, J. N. *Surf. Sci.* **1997**, *373*, 67.

(41) Duchovic, R. J.; Volobuev, Y. L.; Lynch, G. C.; Jasper, A. W.; Truhlar, D. G.; Allison, T. C.; Wagner, A. F.; Garrett, B. C.; Espinosa-Garcia, J.; Corchado, J. C., POTLIB-online, http://comp.chem.umn.edu/potlib.